ACS OMEGA

http://pubs.acs.org/journal/acsodf

Article

Synthesis, Hemolytic Studies, and *In Silico* Modeling of Novel Acefylline−1,2,4-Triazole Hybrids as Potential Anti-cancer Agents against MCF-7 and A549

Irum Shahzadi, Ameer Fawad Zahoor,* Azhar Rasul, Asim Mansha, Sajjad Ahmad, and Zohaib Raza

Cite This: *ACS Omega* 2021, 6, 11943−11953

Read Online

ACCESS | Metrics & More | Article Recommendations | Supporting Information

ABSTRACT: A series of novel theophylline-7-acetic acid (acefylline)-derived 1,2,4-triazole hybrids with *N*-phenyl acetamide moieties (**11a−j**) have been synthesized and tested for their inhibitory (*in vitro*) potential against two cancer cell lines, A549 (lung) and MCF-7 (breast), using MTT assay. Among these derivatives, **11a**, **11c**, **11d**, **11g**, and **11h** displayed remarkable activity against both cancer cell lines having cell viability values in the 21.74 ± 1.60−55.37 ± 4.60% range compared to acefylline (86.32 ± 1.75%) using 100 $\mu g/\mu L$ concentration of compounds. These compounds were further screened against the A549 cancer cell line (lung) to find their half-maximal inhibitory concentration (IC_{50}) by applying various concentrations of these compounds. Compound **11g** (2-(5-((1,3-dimethyl-2,6-dioxo-2,3-dihydro-1*H*-purin-7(6*H*)-yl)methyl)-4-phenyl-4*H*-1,2,4-triazol-3-ylthio)-*N*-*p*-tolylacetamide) with the least IC_{50} value (1.25 ± 1.36 μM) was discerned as a strong inhibitor of cancer cell multiplication in both cell lines (A549 and MCF-7). Their hemolytic studies revealed that all of them had very low cytotoxicity. Finally, *in silico* modeling was carried out to find the mode of binding of the highly active compound (**11g**), which was according to the results of anti-cancer activity.

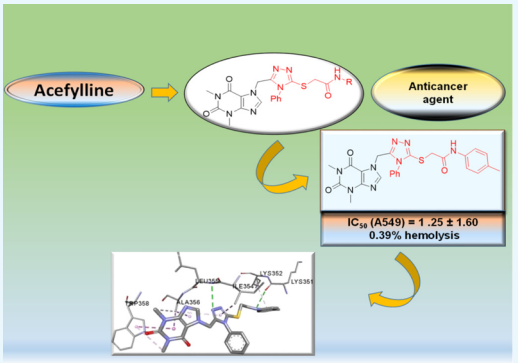

1. INTRODUCTION

Cancer is the second most fatal disease in the world after cardiovascular diseases.[1] Every year, about 7.6 million people die of cancer globally, and this number is expected to reach 13 million by 2030.[2] According to an estimate published by the WHO, the number of new cases is expected to rise by about 70%, that is, from 14 million to 22 million over the next 2 decades. Cancer was responsible for 10 million deaths in 2020. Globally, approximately, 19 million new cases were registered in 2020, and nearly, one out of six deaths is due to cancer and this is projected to increase by 45% (during 2007−2030), killing more people than HIV/AIDS, malaria, and tuberculosis combined. The major organs affected by cancer in men and women include the prostate, breast, lung and bronchus, thyroid, uterine, carpus, colon, and rectum.[3] It is important to note that female breast cancer diagnosis has exceeded with an estimated 2.3 million new cases, that is, 11.7%. It was found to be 11.4% for lung followed by colorectal (10.0%), prostate (7.3%), and stomach (5.6%) cancers. Cancer is currently being treated with chemotherapy, surgery, and radiotherapy. The cancerous cell curability *via* chemotherapy is attributed only to 11%, while surgery accounts for 49% and radiotherapy accounts for 40%. Various chemotherapeutic medicines are in market at very high price and have adverse side effects and low efficacy. Thus, it is one of the leading interests in drug development and discovery to look for novel anti-cancer drugs.[4,5]

In this regard, 1,2,4-triazole-derived heterocycles have gained significant attention in the last few years owing to their chemotherapeutic values.[6,7] The literature reveals that 1,2,4-triazole derivatives hold numerous therapeutic features such as analgesic,[8] anti-microbial,[9,10] local anesthetic, anti-inflammatory,[11] anti-malarial,[12] anti-convulsant,[13] anti-viral,[14] anti-neoplastic,[15] and anti-cancer activities.[16−18] It is important to note that 1,2,4-triazole-containing anti-cancer drugs such as letrazole and anastrozole (Figure 1) are already in use for the treatment of breast cancer.[19]

Similarly, medicinal plants are the basis for exploring different marketing drugs. One of such prominent molecules is xanthine. Different forms of xanthines (theophylline, theobromine, doxophylline, and caffeine, Figure 2)[20] are known for their wide applications in pharmaceutical industry as anti-microbial,[21] anti-inflammatory,[22] anti-oxidant, cyclic

Received: January 23, 2021
Accepted: April 21, 2021
Published: April 30, 2021

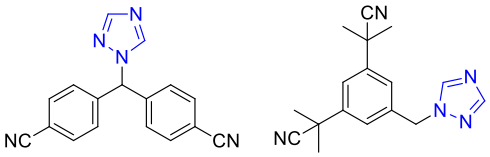

Figure 1. Bioactive 1,2,4-triazole anti-cancer drugs letrazole (**1A**) and anastrozole (**1B**).

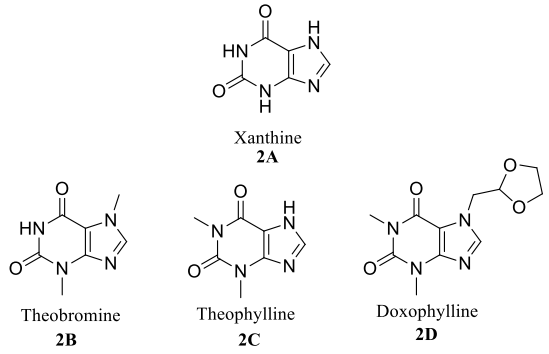

Figure 2. Structures of xanthine (**2A**) and various xanthine derivatives such as theobromine (**2B**), theophylline (**2C**), and doxophylline (**2D**).

nucleotide phosphodiesterase inhibition, adenosine receptor antagonist,[23] and anti-tumor activities.[24]

Theophylline has gained considerable interest among the widely distributed methylxanthines, as it has been the commonly used dimethylxanthine for treating respiratory diseases such as asthma for over 80 years.[25] Theophylline comprises an important scaffold for modifications in the structure to develop CNS stimulant,[26] analgesic and anti-inflammatory,[27,28] anti-bacterial,[29] hypotensive,[30] hypoglycemic,[31] anti-HIV,[32] and anti-cancer[33] derivatives. Theophylline is an appropriate drug used in cardiology for the treatment of bradyarrhythmias and disorder of atrioventricular conduction.[34] Theophylline-7-acetic acid (acefylline, Figure 3), a

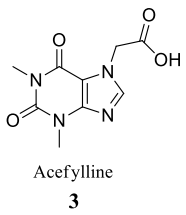

Figure 3. Structure of acefylline.

pharmacologically active derivative of theophylline, is widely used as a bronchodilator, cardiac stimulant, diuretic, and smooth muscle-relaxing agent.[35] Its amide and methyl ester derivatives are active against myeloid leukemia cells,[36] mycobacterium tuberculosis,[37] and cancer cell lines.[38]

Our research group has previously reported some 1,3,4-oxadiazoles derived from acefylline as anti-cancer agents with least toxicity.[39] Considering the chemotherapeutic importance of acefylline and 1,2,4-triazole derivatives and part of our ongoing studies toward novel biologically relevant molecules,[40,41] it has been decided to synthesize 1,2,4 triazole hybrids of acefylline and investigate their cytotoxicity.

2. RESULTS AND DISCUSSION

2.1. Chemistry. Acefylline derivatives were synthesized in various steps, as presented in Scheme 1. Acefylline **3** was esterified with CH_3OH using a catalytic amount of sulfuric acid to afford theophylline-7-acetate **4** in 72% yield, followed by the reaction with hydrazine monohydrate to get 7-acetohydrazide of theophylline **5** in 99% yield.[39] The synthesized theophylline-7-acetohydrazide **5** was further treated with phenyl isothiocyanate in ethanol to prepare thiosemicarbazide **6**, which was hydrolyzed in basic media to obtain acefylline−triazole hybrid **7** in 70% yield.[42] Various aromatic amines **8a−j** were treated with bromo acetyl bromide **9** to obtain 2-bromo-*N*-substitutedphenyl acetamides **10a−j**[43] and were coupled with **7** in dichloromethane to obtain the target compounds in the presence of pyridine **11a−j** in 65−82% yield (Scheme 1, Table 1).

2.2. Spectral Explanation of the Demonstrative Molecule (11c). Acefylline-derived (compound) **11c** was synthesized as a brown amorphous solid, and its structural confirmation was done by IR, ^{1}H-, ^{13}C NMR, and MS-EI spectroscopy (M^+) at m/z: 530.1849. To describe various functional groups in Fourier transform infrared spectroscopy (FTIR), different absorption spectra were seen at ν: 3362 (N−H, str), 1643 (CO−amide, str), 1600−1650 (CO−xanthene, str), 1545 (C═N, str), Ph (1447), 1453 (C═C, str), 1473 (CH_2, str), 1331 (C−N, str), 801 (C−H), and 650−710 (S−C) cm^{-1}. In the ^{1}H NMR spectrum, methylene and NH of the amide group (signals) are seen at δ 4.11 and δ 10.16, respectively. The most downfield signal was detected at δ 8.00 for N−H of the xanthene heterocyclic ring. 2H-4 of the CH_2 group resonated in the upfield region at δ 5.58, whereas 3H-1 and 3H-2 of the purine ring resonated at δ 3.14 and δ 3.41 as a singlet. The presence of two methyl groups at the aromatic ring (CH_3-2′ and CH_3-4′) was confirmed by two signals at δ 2.15 and δ 2.17, respectively. *H*-5′ and *H*-6′ (aromatic protons) reverberated at δ 7.06 (J = 6.4 Hz) as a doublet and at δ 7.25 (J = 7.1 Hz), respectively, while *H*-3′ reverberated as a singlet at δ 7.31. At δ 7.48; two aromatic protons *H*-9′ and *H*-11′ resonated as a multiplet, while *H*-8′ and *H*-12′ appeared at δ 7.58 (J = 1.9 Hz) with *H*-7′ and *H*-11 as a doublet, respectively. H-10′ of the aromatic ring appeared as a triplet at δ 7.58 and showed *ortho* couplings with *H*-9′ and *H*-11′ (Figure 4A).

The carbon framework of **11c** was also confirmed by ^{13}C NMR. In the spectrum, all of the 26 carbons showed their signals; two resonance signals at δ 37.29 for the methylene group and at δ 165.43 for the carbonyl group confirmed the N-substituted acetamide group. The other two signals belonged to 2 C═O of the purine ring at δ 151.77 and 154.63. Formation of the 1,2,4 triazole ring was confirmed by the downfield signals depicted by quaternary carbons at δ 151.36 and δ 151.70. One signal of methine at δ 143.51 and the two signals of C═C at δ 106.46 and 148.40 exhibited the presence of theophylline ring in the molecule. The signal of the methylene linker between the theophylline and 1,2,4 triazole core appeared at δ 41.33. The 2,4-dimethylphenyl ring attached with the acetamide group showed three methine signals at δ 130.76, δ 120.78, and δ 117.12, while the other three signals of substituted phenyl carbons were seen at δ 136.81 and δ 132.40 for C−CH_3 and δ 131.73 for C−N. Two methyl substituents at the phenyl ring were seen in the upfield region of the spectrum at δ 2.15 and δ 2.17. The phenyl ring

https://doi.org/10.1021/acsomega.1c00424
ACS Omega 2021, 6, 11943−11953

Scheme 1. Reaction Conditions and Pathway for the Synthesis of Target Compounds (11a−j)[a]

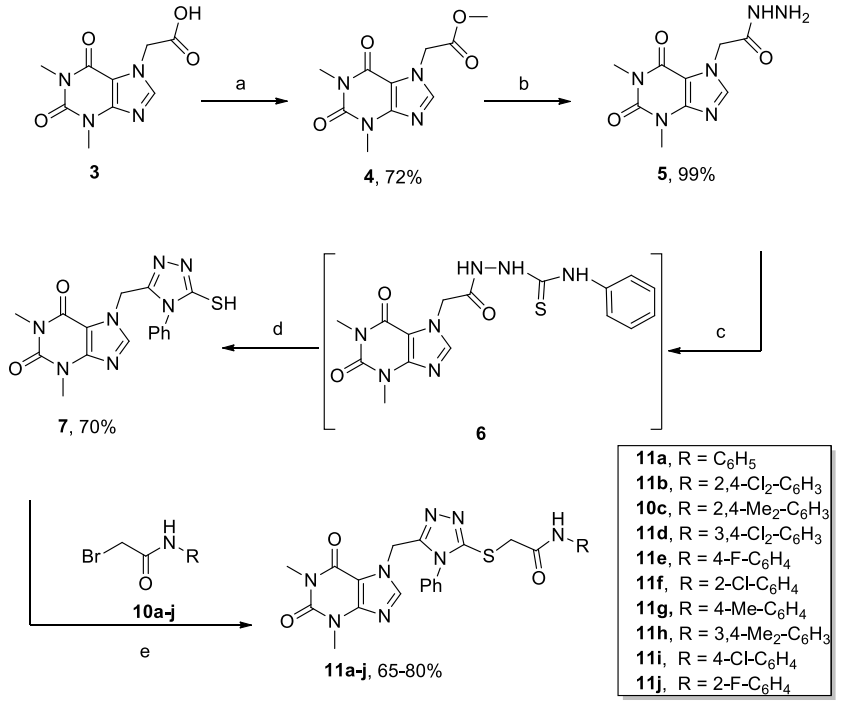

[a]Reagents and conditions of reactions: (a) methanol, H_2SO_4, reflux 6 h. (b) Hydrazine monohydrate, RT overnight. (c) Phenyl isothiocyanate, C_2H_5OH, RT 1 h, reflux 2 h (d) Aq KOH, heat 4 h (e) DCM, pyridine, RT 24−48 h.

joined with 1,2,4-triazole was confirmed by one downfield signal of C−N at δ 136.93 and two signals for C-8′ and C-12′ resonated at δ 130.45 and δ 130.06, respectively, while the remaining three carbons of the phenyl ring depicted their signals at δ 127.46 (Figure 4B). By a similar approach, other synthetic derivatives of the series (**11a−j**) were also structurally characterized.

2.3. Anti-cancer Activity. The cytotoxic prospective of all the target compounds **11a−j** was reviewed against two cancer cell lines, MCF-7 (human breast) and A549 (lung), and found to have lower cell viability values (100 μg/μL) as compared to the reference drug acefylline (86.32 ± 11.75%) using 100 μg/μL concentration of the compound (Table 1). In general, compounds **11a**, **11c**, **11d**, **11g**, and **11h** showed greater activity with both tested cancer cell lines. Compounds **11c** (cell viability = 38.74 ± 2.07, 26.14 ± 1.86%) and **11g** (cell viability = 31.76 ± 3.16, 21.74 ± 1.60%) for MCF-7 (breast) and A549 (lung) were preferably established more effectively against the lung cancer cell line (A549). The half-maximal inhibitory concentration (IC_{50}) for these compounds was also calculated against the lung cancer cell line A549 applying different concentrations of compounds. All the compounds showed good inhibition potential. **11g** with the IC_{50} value 1.25 ± 1.36 μM was considered a potent anti-cancer derivative among all. Compounds **11e** and **11i** also exhibited moderate cytotoxic activity with cell viability (54.82 ± 4.88, 52.07 ± 3.66 and 50.82 ± 2.78, 52.477 ± 2.59%), but the compounds **11b**, **11f**, and **11j** with relatively high values of cell viability were considered least active against cancer.

2.4. Hemolytic Activity. The acefylline-derived analogues (**11a−j**) were also verified for hemolytic assay. The %age of hemolysis was deliberated, and the data are displayed in Table 1. Synthesized derivatives revealed low toxicity with RBCs. Least toxicity was detected for molecule **11g** (0.39%), which showed minimum binding with the RBC cell membrane as compared to standard ABTS (95.9% hemolysis). The most toxic compound was found to be derivative **11b** with hemolysis (15%), whereas all other derivatives, **11a** (11.7), **11f** (8.6%), **11d** (5.5%), **11j** (4.6%), **11h** (5.9%), and **11i** (8.9%), exhibited moderate to low hemolytic activity.

2.5. Structure−activity Relationship. SAR (structure−activity relationship) was investigated depending on substituents on the phenyl ring of *N*-(substituted-phenyl)-acetamide to obtain all the comprehensive facts about anti-cancer activities of synthesized molecules. An understanding about the structures and activities of the compounds under examination suggests that incorporating substituents with the electron-donating effect usually increased the anti-cancer activity, for example, compound **11a** possessing the unsubstituted phenyl ring of acetanilides exhibited greater activity (34.73 ± 2.49, 59.59 ± 1.36%) against MCF-7 and A549 cancer cell lines as compared to the reference drug acefylline (86.32 ± 11.75%). Substituted phenyl rings with electron-donating groups at different positions exhibited remarkable results. Compound **11g** bearing the methyl group on the phenyl ring at the *para* position showed excellent anti-cancer activity (cell viability = 31.76 ± 3.16, 21.74 ± 1.60%) among all the synthetic derivatives. The activity was slightly decreased in dimethyl-substituted derivatives, such as that compound **11h** (cell viability = 33.20 ± 2.77, 55.37 ± 4.60%) was the second most active derivative of the series with two methyl groups adjacently attached on the phenyl ring at *meta* and *para* positions. However, the adjustment in the position of methyl groups at *ortho* and *para* resulted in a decrease in the activity of compound **11c** (cell viability = 38.74 ± 2.07, 26.14 ± 1.86%). This suggests that the presence of the electron-donating substituent in the phenyl ring at *para* and *meta* positions

https://doi.org/10.1021/acsomega.1c00424
ACS Omega 2021, 6, 11943−11953

Table 1. Anti-cancer and Hemolytic Potential of Thio *N*-(Substituted-phenyl)acetamide Derivatives of Theophylline-7-acetic Acid (Acefylline) 11a−j

Compounds	-R	*Cell viability (%) MCF-7 (breast)	*Cell viability (%) A549 (lung)	IC_{50} (μM) A549 (lung)	% Hemolysis
11a		34.73 ± 2.49	59.59 ± 1.36	143.12 ± 1.36	11.7
11b	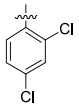	69.40 ± 7.05	52.60 ± 5.07	-	15
11c	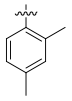	38.74 ± 2.07	26.14 ± 1.86	7.39 ± 1.86	2.7
11d	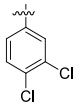	38.14 ± 4.04	46.21 ± 1.42	80.59 ± 1.42	5.5
11e	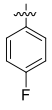	54.82 ± 4.88	52.07 ± 3.66	-	2.1
11f		72.78 ± 6.35	55.43 ± 4.11	-	8.6
11g	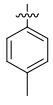	31.76 ± 3.16	21.74 ± 1.60	1.25 ± 1.60	0.39
11h	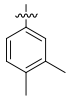	33.20 ± 2.77	55.37 ± 4.60	197.8 ± 4.60	3.9
11i	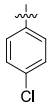	50.82 ± 2.78	52.47 ± 2.59	-	7.2
11j		63.72 ± 3.54	67.54 ± 4.27	-	4.6
Acefylline		86.32 ± 11.75	-	-	43.5
Control (DMSO)		100 ± 0			
ABTS					95.39

[a]Cell viability, IC_{50}: (Mean ± SD) in triplicate.

compared to that in *ortho* may be more interactive with the cancer cells and is the reason of its greater potential (Figure 5).

The activity of compound **11d** (cell viability = 38.14 ± 4.04, 46.21 ± 1.42%) bearing two chloro groups at *meta* and *para* positions showed considerable activity, while the activity was decreased when the position of chloro groups was changed to *ortho* and *para* in structurally similar hybrids such as **11i** (50.82 ± 2.78 ± 52.47 ± 2.59%) and **11b** (cell viability = 69.40 ± 7.05, 52.60 ± 5.07%). Compound **11f** (cell viability = 72.78 ± 6.35, 55.43 ± 4.11%) having the mono-substituted *ortho*

https://doi.org/10.1021/acsomega.1c00424
ACS Omega 2021, 6, 11943−11953

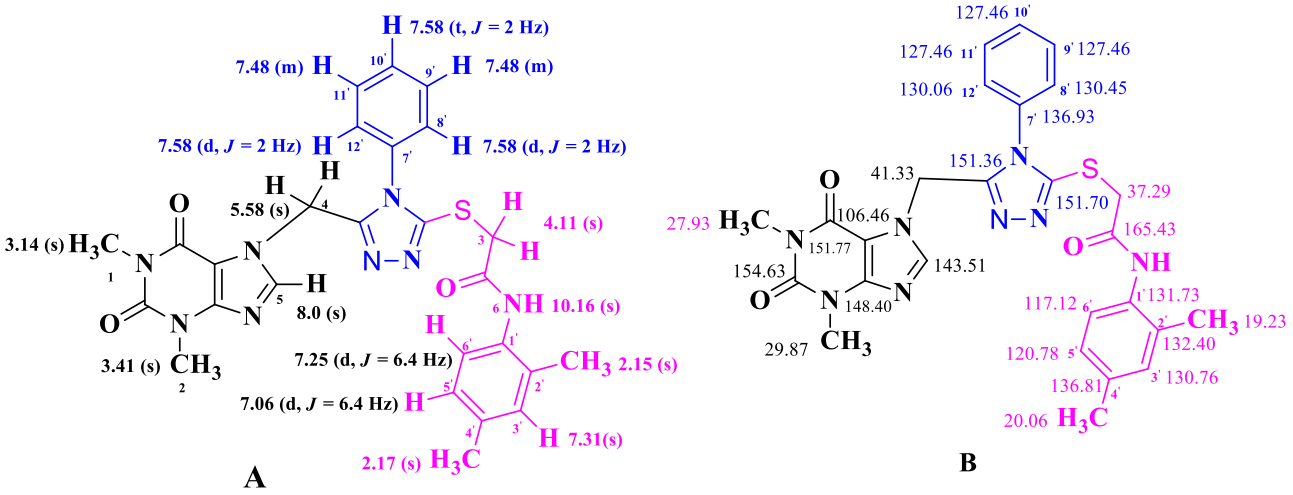

Figure 4. ^{1}HNMR (A) and ^{13}C NMR (B) of the compound **11c**.

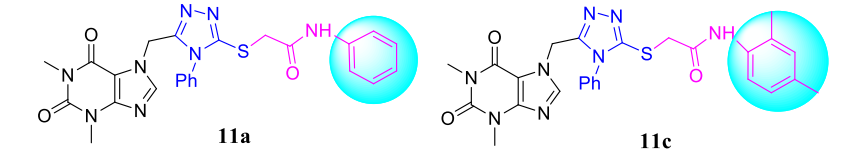

Cell viability = (34.73 ± 2.49%, 59.59 ± 1.36%) Cell viability = (38.74 ± 2.07%, 26.14 ± 1.86%)

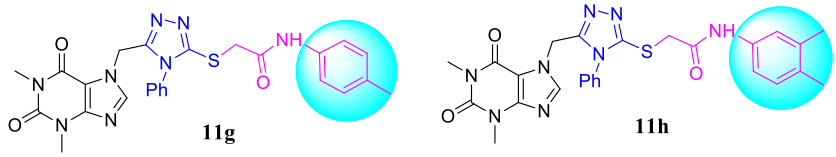

Cell viability = (31.76 ± 3.16%, 21.74 ± 1.60%) Cell viability = (33.20 ± 2.77%, 55.37 ± 4.60%)

Figure 5. SAR of **11a**, **11c**, **11g**, and **11h**.

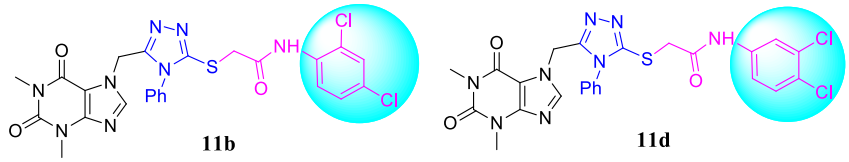

Cell viability = (69.40 ± 7.05%, 52.60 ± 5.07%) Cell viability = (38.14 ± 4.04%, 46.21 ± 1.42%)

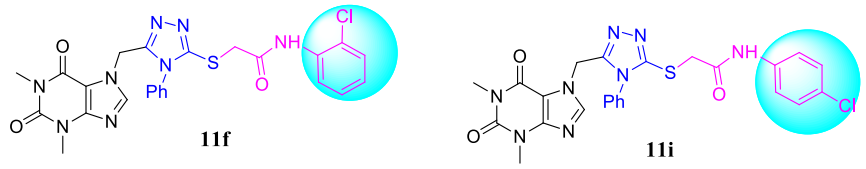

Cell viability = (72.78 ± 6.35%, 55.43 ± 4.11%) Cell viability = 50.82 ± 2.78%, 52.47 ± 2.59%

Figure 6. SAR of **11b**, **11d**, **11f**, and **11i**.

chloro phenyl ring showed less inhibitory potential toward the MCF-7 (human breast) cancer cell line and found to be least active among all the derivatives (Figure 6).

Compound **11e** (cell viability = 54.82 ± 4.88, 52.07 ± 4.88%) with the fluoro group at the *para* position of the phenyl group also showed moderate activity, while the activity of compound **11i** (cell viability = 63.72 ± 3.54, 67.54 ± 4.27%) bearing the fluoro substituent at the *ortho* position was decreased (Figure 7). It is obvious from the results that the presence of an electron-donating substituent in the phenyl ring at *para* and *meta* positions as compared to that in *ortho* increased the activity of compounds, while the activity was

https://doi.org/10.1021/acsomega.1c00424
ACS Omega 2021, 6, 11943−11953

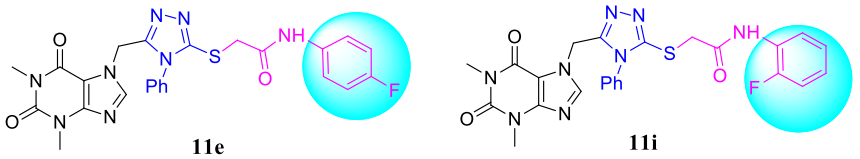

Figure 7. SAR of compounds **11e** and **11i**.

decreased when an electron-withdrawing substituent is present at the *ortho* position.

The same trend was observed in hemolytic activity; compounds having a electron-donating substituent on the phenyl ring—**11g**, **11c**, and **11h** (0.39, 2.7, and 3.9%, respectively)—are less toxic, while compounds bearing an electron-withdrawing substituent on the phenyl ring—**11b**, **11d**, **11f**, and **11i** (15, 5.5, 8.6, and 7.2%, respectively) and unsubstituted phenyl ring, **11a** (17%), with greater hemolytic activity are more toxic.

2.6. Computational Modeling Studies of the Most Active Compound (11g). *2.6.1. Results.* The compounds were computationally modeled to explore their mechanism of action in cancer. The PASS tool predicted the STAT3 as a potential anti-cancer target with Pa ∼ 0.614. STAT3 is a vital transcript factor that regulates the cell propagation, differentiation, and survival. It has been reported that theophylline modulates the STAT3 signaling, and STAT3 dimerization inhibition is a potential therapeutic modality to control the progression, development, and conservation of malignancies.[44−47] Herein, the inhibitory potential of compound **11g** was studied by induced fit docking. The **11g** docked at the STAT3 hotspot with a superior conformational energy of −6.2789 Kcal/mol. It was found to significantly exceed the standard's threshold of conformational energy (*i.e.*, −4.6825 Kcal/mol), which suggested the improved STAT3 inhibitory potential of **11g** as compared to acefylline (Table 2).

Table 2. Parameters for Induced-Fit Docking of Compounds at the STAT3 Hotspot

compounds	binding score (ΔG) Kcal/mol	binding Residues	interactions type
11g	−6.2789	TRP358. ALA356, ILE354, LEU355, LYS351, LYS352	H-bonding, π−π stacking, π−σ, alkyl,π-alkyl
acefylline	−4.6825	TYR353, LYS351, THR151, ILE354, LEU355, LYS352, VAL350	H-bonding, π−σ, alkyl, π-alkyl

The binding pocket consists of THR150, THR151, CYC152, LYS352, TYR353, ILE354, LEU355, and ALA356 at the hotspot of STAT3. Acefylline was found to orient itself at the STAT3 hotspot and stabilized its conformation by contacts with vital residues to disrupt the STAT3 interactions (Figure 8),[39] whereas conformational analysis of **11g** revealed that it preferably binds with STAT3 to block its complexation at the hotspot. Interestingly, conformation of **11g** was able to interact with all STAT3 residues at the binding pocket, which may disrupt the formation of the hotspot during STAT3 complexation.

Acefylline was found to stabilize its complexation by H-bonding with LYS351, TYR353, ILE354, and LEU355. It also established the alkyl and pi-alkyl interactions with ILE354, VAL350, and LYS352. Moreover, it also interacted with THR151 by a pi-sigma bond at the STAT3-binding site (Figure 9). On the other hand, **11g** efficiently interacted with conserved residues of acefylline but with higher binding affinity. The compound **11g** complexed and inhibited the STAT3 hotspot by strong hydrogen bonds with LEU355 and LYS351. It also formed the Pi-alkyl bonds with LYS352, pi-alkyl, and pi−pi stacked bonds with TRP358 and an alkyl bond with ALA356. Additionally, compound **11g** further supported this complexation by pi-sigma bonds with ALA356 and ILE354. It is noteworthy that **11g** established the diverse interactions with STAT3 residues and disrupted its complexation at the hotspot, thus corroborating its superior binding energy and inhibitory potential.

The two-dimensional (2D) illustration of acefylline (A) and derivative **11g** (B) interacting with STAT3-binding pocket residues represented as colored balls by kind of collaboration is provided.

2.6.2. Discussion. The compound **11g** was computationally modeled to investigate its superior anti-cancer potential as compared to acefylline. Herein, the PASS predication highlighted the STAT3 as a potential anti-cancer target for **11g**. The superior binding affinity of the compound under examination was investigated by the function of induced fit docking with acefylline as a standard. It is a reliable methodology that accounts for the stretchy receptor' binding pocket to simulate and predicts the binding mode and complexation of the ligand. Interestingly, compound **11g** conformed with higher binding affinity, which may justify its improved anti-cancer potential as compared to acefylline. Moreover, compound **11g** efficiently oriented itself toward the STAT3 hotspot and inhibited the STAT3 residues with more diverse interactions, which may completely disrupt the STAT3 potential of complexation. Therefore, these insights may further support the compound **11g** as a novel acefylline-based lead candidate in cancer therapeutics.

3. CONCLUSIONS

The targeted compounds thio *N*- phenyl/arylacetamide derivatives of acefylline **11a−j** were synthesized in good yield. The anti-cancer activity of all derivatives was screened against cell lines of cancer, MCF-7 (breast) and A549 (lung), and it was revealed that most compounds exhibited better anti-proliferative activity. Among these compounds, **11g** with the least IC_{50} value (1.25 ± 1.60 μM) was recognized to be the most potent agent against both cancer cell lines. Almost all molecules showed low cytotoxicity against human RBCs in the hemolysis assay. The mode of action in the inhibition of cancer cells of the compound **11g** was also examined by docking studies, and the results of comprehensive docking analysis of compound **11g** are consistent with biological diagnostic findings. Overall, current studies suggest that acefylline-linked

https://doi.org/10.1021/acsomega.1c00424
ACS Omega 2021, 6, 11943−11953

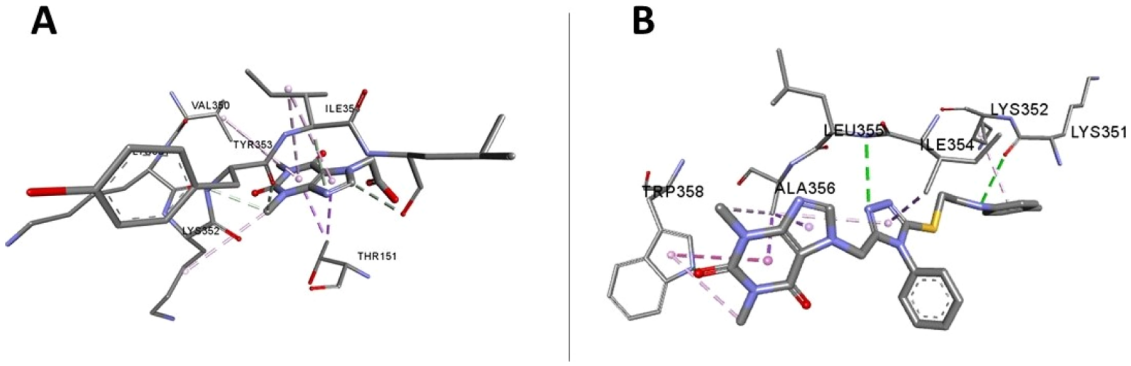

Figure 8. Conformational analysis of docked compounds at the STAT3-binding pocket. Spatial configuration of the simulated greatest binding approach of A (acefylline) and B (**11g**) at the 3D space of the interacted place for STAT3.

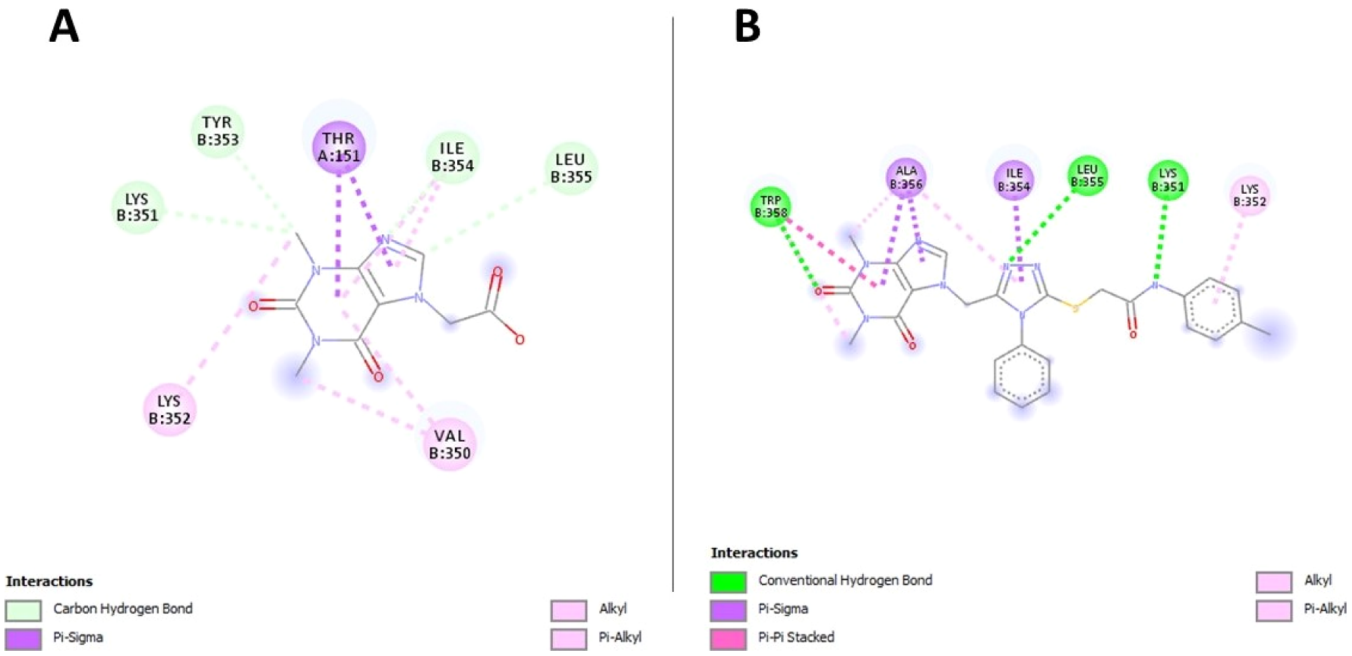

Figure 9. Docked compounds interacting with the residues of the STAT3-binding pocket.

triazole hybrids are capable of being established as lead compounds; more modifications on triazole derivatives of acefylline may give rise to advanced anti-cancer agents in cancer therapy.

4. MATERIALS AND METHODS

4.1. Chemistry. Starting materials, chemicals, and solvents of analytical grade were obtained from local traders from Alfa Aesar, Merck, and Sigma-Aldrich (Germany) and were used without distillation. Thin-layer chromatography (TLC) was performed to monitor the reaction using silica gel plates coated with 60 F254 in a mixture of methanol and dichloromethane. UV light was used to detect the spots on TLC plates. Melting points (mp) were noted using *Gallenkamp* equipment. FTIR spectra were documented on a Bruker FTIR spectrometer in KBr pellets. The spectra of ^{1}H NMR and ^{13}C NMR at 400 MHz and 100 MHz (δ = ppm), respectively, in DMSO-d_6 were documented on a Bruker model *AV-400* spectrophotometer.

4.2. Synthesis of 7-((5-mercapto-4-phenyl-4*H*-1,2,4-triazol-3yl)methyl)-1,3-dimethyl-1*H*-purine-2,6(3*H*,7*H*)-dione (7). To the mixture of theophylline acetohydrazide **5** (300 mg, 1.2 mmol) in ethanol (20 mL) was added phenyl isothiocyanate (162 mg, 1.2 mmol) and placed for 1 h; later, the brew was refluxed for 2 h. Precipitates of thiosemicarbazide (intermediate) **6** were formed, which were filtered off and dried. The intermediate was then dissolved in a solution of KOH (0.1 mg, 1.8 mmol) in H_2O (5 mL). The mixture was then heated for 4 h in a water bath. It was then cooled and acidified with dilute HCl; precipitates were filtered out and purified by a recrystallization process as a white solid. Yield: 70%; mp 287 °C; IR ν: 3290 (H−Ar), 2500−2600, (S−H), 1605−1652 (2C═O), 1550 (C═C), 1550 (N═C), 1472 (CH_2), 600−700 (S−C). ^{1}H NMR, DMSO-d_6, 400 MHz (δ/ppm): 1.6 (s, S−*H*), 3.22, 3.30 (s, 6H, 2*N*−CH_3), 5.79 (s, 2H, *N*−CH_2), 8.20 (s, 1H, CH═N). ^{13}C NMR, DMSO-d_6, 100 MHz (δ/ppm): 28 (CH_3), 29.6 (CH_3), 43, (NCH_2), 107, 123, 132, 143, 147, (Ar−C), 153.2, 154.9 (CO−xanthine).

4.3. General Synthetic Procedure for the Compounds (11a−j). To the mixture of 1,2,4-triazoles analogue **7** (200 mg, 0.54 mmol) and dichloromethane and pyridine (1.89 mmol) were added 2-bromo-*N*-phenylacetamides **10a−j** (2.4 mmol), and the resulting mixture was stirred at room temperature for 24−48 h. Reaction was monitored with the help of TLC. Upon reaction completion, *n*-hexane was added, and precipitates of

https://doi.org/10.1021/acsomega.1c00424
ACS Omega 2021, 6, 11943−11953

N-substituted phenylacetamide analogues of 1,2,4-triazole−acefylline hybrid **11a−j** were obtained, which were recrystallized with ethanol.

*4.3.1. 2-(5-((1,3-Dimethyl-2,6-dioxo-2,3-dihydro-1H-purin-7(6H)-yl)methyl)-4-phenyl-4H-1,2,4-triazol-3-ylthio)-N-phenylacetamide (**11a**).* Light-yellow powder; yield: 75%; mp 210 °C; IR (KBr) ν: 1600−1650 (2C═O), 3351 (N−H), 1643 (CONH), 1545 (N═C), 1473 (CH_2), Ph (1476), 1453 (C═C), 1331 (N−C), 600−700 (S−C), 801 (Ar−H). ^{1}H NMR, DMSO-d_6, 400 MHz (δ/ppm): 3.15, 3.41 (s, 6H, *N*−CH_3), 4.15 (s, 2H, *S*-methylene), 5.58 (s, 2H, *N*-methylene), 7.06 (t, $J_{4',5/4',3'}$ = 5.6 Hz, 1H, *H*-4′), 7.30 (t, $J_{3',2}$ = $J_{5',6''}$ = 6 Hz, 2H, *H*-3′, 5′), 7.48 (d, $J_{8',9'}$ = $J_{11',12'}$ = 5.8 Hz, 2H, *H*-8′, 12′), 7.55 (d, $J_{2',3'}$ = $J_{5',6'}$ = 6.2 Hz, 2H, *H*-2′, 6′), 7.58 (m, 3H, *H*-9′, 10′, 11′), 8.0 (s, 1H, HC═N), 10.32 (s, 1H, CO−amide).^{13}C NMR, DMSO-d_6, 100 MHz (δ/ppm): 27.93 (methyl), 29.90 (methyl), 37.41 (*S*-methylene), 41.36, (*N*-methylene), 106.50, 119.56, 121.09, 123.99, 127.46−132.42 (11C), 139.20, 143.52 (2C), 148.41, 151.37, 151.64 (Ar−C), 151.80, 154.63 (2CO−xanthene), 165.78 (CO−amide). ES$^+$ MS (*m*/*z* %): 502.1536 (M^+). Anal. Calcd for $C_{24}H_{22}N_8O_3S$: C, 56.95; H, 4.48; N, 21.96. Found: C, 57; H, 4.41; N, 22.30.

*4.3.2. N-(2,4-Dichlorophenyl)-2-(5-((1,3-dimethyl-2,6-dioxo-2,3-dihydro-1H-purin-7(6H)-yl)methyl)-4-phenyl-4H-1,2,4-triazol-3-ylthio)acetamide (**11b**).* Pale-yellow solid; yield: 72%; mp 223 °C; IR (KBr) ν: 1600−1650 (2C═O), 3351 (N−H), 1643 (CONH), 1545 (N═C), 1453 (C═C), 1331 (N−C), 600−700 (S−C), 801 (Ar−H), 1473 (CH_2), Ph (1456). ^{1}H NMR, DMSO-d_6, 400 MHz (δ/ppm): 3.15, 3.41 (s, 6H, *N*−CH_3), 4.14 (s, 2H, *S*-methylene), 5.57 (s, 2H, *N*-methylene), 7.49−7.59 (m, 7H, Ar−H), 7.93 (s, 1H, *H*-3), 8.0 (s, 1H, HC═N), 10.64 (s, 1H, CO−amide). ^{13}C NMR, DMSO-d_6, 100 MHz (δ/ppm): 27.93 (methyl), 29.90 (methyl), 37.19 (*S*-methylene), 41.31, (*N*-methylene), 106.50, 119.61, 120.67, 127.41, 130.47−132.35 (7C), 139.27, 143.45 (2C), 148.39, 149.29, 151.43 (Ar−C), 151.85, 154.63 (2CO−xanthene), 166.39 (CO−amide). ES$^+$ MS (*m*/*z* %): 570.0756 (M^+). Anal. Calcd for $C_{24}H_{20}Cl_2N_8O_3S$: C, 50.35; H, 3.60; N, 19.53. Found: C, 50.44; H, 4; N, 19.61.

*4.3.3. 2-(5-((1,3-Dimethyl-2,6-dioxo-2,3-dihydro-1H-purin-7(6H)-yl)methyl)-4-phenyl-4H-1,2,4-triazol-3-ylthio)-N-(2,4-dimethylphenyl)acetamide (**11c**).* Brown solid; yield: 69%; mp 112 °C; IR (KBr) ν: 1600−1650 (2C═O), 3351 (N−H), 1643 (CONH), 1545 (N═C), 1473 (CH_2), Ph (1476), 1453 (C═C), 1331 (N−C), 600−700 (S−C), 801 (Ar−H). ^{1}H NMR, DMSO-d_6, 400 MHz, (δ/ppm): 2.15, 2.17 (6H, Ar−CH_3), 3.14, 3.41 (s, 6H, *N*−CH_3), 4.11 (s, 2H, *S*-methylene), 5.58 (s, 2H, *N*-methylene), 7.06 (d, $J_{5',6'}$ = 6.4 Hz, 1H, *H*-5′), 7.25 (d, $J_{6',5'}$ = 6.4 Hz, 1H, *H*-6′), 7.31 (s, 1H, *H*-3′), 7.48 (m, 2H, *H*-9′, 11′), 7.58 (t, J10′,9′′/J10′,11′′ = 2 Hz, 1H, *H*-10′), 7.58 (d, J8′,7′′ = J11′,12′′ = 2 Hz, 2H, *H*-8′, 12′), 8.0 (s, 1H, HC═N), 10.16 (s, 1H, CO−amide). ^{13}C NMR, DMSO-d_6, 100 MHz, (δ/ppm): 19.23 (methyl), 20.06 (methyl), 27.93 (methyl), 29.87 (methyl), 37.29 (*S*-methylene), 41.33, (*N*-methylene), 106.46, 117.12, 120.78, 127.46 (3C), 130.06, 130.45, 130.76, 131.73, 132.40, 136.81, 136.93, 143.51, 148.40, 151.36, 151.70 (Ar−C), 151.77, 154.63 (2CO−xanthene), 165.43 (CO−amide). ES$^+$ MS (*m*/*z* %): 530.1849 (M^+). Anal. Calcd for $C_{26}H_{26}N_8O_3S$: C, 50.35; H, 3.60; N, 19.53. Found; C, 58.85; H, 4.94; N, 21.12.

*4.3.4. N-(3,4-Dichlorophenyl)-2-(5-((1,3-dimethyl-2,6-dioxo-2,3-dihydro-1H-purin-7(6H)-yl)methyl)-4-phenyl-4H-1,2,4-triazol-3-ylthio)acetamide (**11d**).* Pale-yellow solid; yield: 71%; mp 222 °C; IR (KBr) ν: 1600−1650 (2C═O), 3351 (N−H), 1643 (CONH), 1545 (N═C), 1473 (CH_2), Ph (1476), 1453 (C═C), 1331 (N−C), 600−700 (S−C), 801 (Ar−H). ^{1}H NMR, DMSO-d_6, 400 MHz, (δ/ppm): 3.15, 3.41 (s, 6H, *N*−CH_3), 4.14 (s, 2H, *S*-methylene), 5.57 (s, 2H, *N*-methylene), 7.44 (t, $J_{9',10/10',11'}$ = 2 Hz, 1H, *H*-10′), 7.48 (d, $J_{8',9}$ = $J_{12',11'}$ = 5.6 Hz, 2H, *H*-8′, 12′), 7.58 (m, 4H, *H*-5′, 6′, 9′, 11′), 8.0 (s, 1H, HC═N), 10.64 (s, 1H, CO−amide). ^{13}C NMR, DMSO-d_6, 100 MHz, (δ/ppm): 27.93 (methyl), 29.90 (methyl), 37.23 (S-methylene), 41.37, (*N*-methylene), 106.50, 119.64, 120.77, 127.44, 130.47−132.38 (7C), 139.27, 143.52 (2C), 148.41, 151.37, 151.44 (Ar−C), 151.86, 154.63 (CO−xanthene), 166.43 (CO−amide). ES$^+$ MS (*m*/*z* %): 570.0756 (M^+). Anal. Calcd for $C_{24}H_{20}Cl_2N_8O_3S$: C, 50.35; H, 3.60; N, 19.53. Found; C, 50.44; H, 3.53; N, 19.61.

*4.3.5. 2-(5-((1,3-Dimethyl-2,6-dioxo-2,3-dihydro-1H-purin-7(6H)-yl)methyl)-4-phenyl-4H-1,2,4-triazol-3-ylthio)-N-(4-fluorophenyl)acetamide (**11e**).* Light-yellow powder; yield: 66%; mp 168 °C; IR (KBr) ν: 1600−1650 (2C═O), 3351 (N−H), 1643 (CONH), 1545 (N═C), 1473 (CH_2), Ph (1476), 1453 (C═C), 1331 (N−C), 600−700 (S−C), 801 (Ar−H). ^{1}H NMR, DMSO-d_6, 400 MHz, (δ/ppm): 3.14, 3.41 (s, 6H, *N*−CH_3), 4.13 (s, 2H, *S*-methylene), 5.58 (s, 2H, *N*-methylene), 7.14 (d, $J_{3',2'}$ = $J_{5',6'}$ = 7.2 Hz, 2H, *H*-3′, 5′),7.48 (d, $J_{2',3'}$ = $J_{6',5'}$ = 2.8 Hz, 2H, *H*-2′, 6′), 7.58 (m, 5H, *H*-8′, 9′, 10′, 11′, 12′), 8.0 (s, 1H, HC═N), 10.40 (s, 1H, CO−amide). ^{13}C NMR, 100 MHz, DMSO-d_6, (δ/ppm): 27.93 (methyl), 29.90 (methyl), 37.41 (*S*-methylene), 41.36, (*N*-methylene), 106.50, 119.56, 121.09, 123.99, 127.46−132.42 (11C), 139.20, 143.52 (2C), 148.41, 151.37, 151.64 (Ar−C), 151.80, 154.63 (2CO−xanthene), 165.78 (CO−amide). ES$^+$ MS (*m*/*z* %): 520.1441 (M^+). Anal. Calcd for $C_{24}H_{22}FN_8O_3S$: C, 55.35; H, 3.90; N, 21.33. Found; C, 55.38; H, 4.07; N, 21.53.

*4.3.6. N-(2-Chlorophenyl)-2-(5-((1,3-dimethyl-2,6-dioxo-2,3-dihydro-1H-purin-7(6H)-yl)methyl)-4-phenyl-4H-1,2,4-triazol-3-ylthio)acetamide (**11f**).* Off-white solid; yield: 70%; mp 117 °C; IR (KBr) ν: 1600−1650 (2C═O), 3351 (N−H), 1643 (CONH), 1545 (N═C), 1473 (CH_2), Ph (1476), 1453 (C═C), 1331 (N−C), 600−700 (S−C), 801 (Ar−H). ^{1}H NMR, DMSO-d_6, 400 MHz, (δ/ppm): 3.15, 3.42 (s, 6H, *N*−CH_3), 4.19 (s, 2H, *S*-methylene), 5.58 (s, 2H, *N*-methylene), 7.19 (t, $J_{3',4'/4',5'}$ = 5.6 Hz, 1H, *H*-4′), 7.32 (t, $J_{5',6'/4',5'}$ = 6 Hz, 1H, *H*-5′), 7.48−7.58 (m, 6H, Ar−*H*), 7.76 (d, $J_{5',6'}$ = 6 Hz, 1H, *H*-6′), 8.0 (s, 1H, HC═N), 9.89 (s, 1H, CO−amide). ^{13}C NMR, DMSO-d_6, 100 MHz, (δ/ppm): 27.93 (methyl), 29.90 (methyl), 37.41 (*S*-methylene), 41.36, (*N*-methylene), 106.50, 119.56, 121.09, 123.99, 127.46−132.42 (11C), 139.20, 143.52 (2C), 148.41, 151.37, 151.64 (Ar−C), 151.80, 154.63 (2CO−xanthene), 165.78 (CO−amide). ES$^+$ MS (*m*/*z* %): 536.1146 (M^+). Anal. Calcd for $C_{24}H_{22}ClN_8O_3S$: C, 50.61; H, 3.88; N, 20.69. Found; C, 53.68; H, 3.94; N, 20.87.

*4.3.7. 2-(5-((1,3-Dimethyl-2,6-dioxo-2,3-dihydro-1H-purin-7(6H)-yl)methyl)-4-phenyl-4H-1,2,4-triazol-3-ylthio)-N-p-tolylacetamide (**11g**).* Light-brown solid; yield: 73%; mp 141 °C; IR (KBr) ν: 1600−1650 (2C═O), 3351 (N−H), 1643 (CONH), 1545 (N═C), 1473 (CH_2), Ph (1476), 1453 (C═C), 1331 (N−C), 600−700 (S−C), 801 (Ar−H), 1473 (CH_2), Ph (1445).^{1}H NMR, DMSO-d_6, 400 MHz, (δ/ppm): 2.23 (s, 3H, Ar−CH_3), 3.15, 3.41 (s, 6H, *N*-methyl), 4.0 (s, 2H, *S*-methylene), 5.57 (s, 2H, *N*-methylene), 7.12 (d, $J_{3',2'}$ = $J_{5',6'}$ = 6.4 Hz, 2H, *H*-3′, 5′), 7.58 (m, 5H, *H*-8′, 9′, 10′, 11′, 12′), 7.47 (d, $J_{2',3'}$ = $J_{6',5'}$ = 3.6 Hz, 2H, *H*-2′, 6′), 8.0 (s, 1H, HC═N), 10.31 (s, 1H, CO−amide). ^{13}C NMR, DMSO-d_6,

https://doi.org/10.1021/acsomega.1c00424
ACS Omega 2021, 6, 11943−11953

100 MHz, (δ/ppm): 20.92 (methyl), 27.92 (methyl), 30.91 (methyl), 37.41 (*S*-methylene), 41.37, (*N*-methylene), 106.53−151.78 (Ar−C), 154.65, 162.09 (CO−xanthene), 164.97 (CO−amide). ES$^+$ MS (m/z %): 536.1146 (M$^+$). Anal. Calcd for $C_{24}H_{22}ClN_8O_3S$: C, 50.61; H, 3.88; N, 20.69. Found; C, 53.68; H, 3.94; N, 20.87.

*4.3.8. 2-(5-((1,3-Dimethyl-2,6-dioxo-2,3-dihydro-1H-purin-7(6H)-yl)methyl)-4-phenyl-4H-1,2,4-triazol-3-ylthio)-N-(3,4-dimethylphenyl)acetamide (**11h**).* Light-gray solid; yield: 67%; mp 148 °C; IR (KBr) ν: 1600−1650 (2C═O), 3351 (N−H), 1643 (CONH), 1545 (N═C), 1473 (CH_2), Ph (1476), 1453 (C═C), 1331 (N−C), 600−700 (S−C), 801 (Ar−H). ^{1}H NMR, DMSO-d_6, 400 MHz, (δ/ppm): 2.17 (6H, Ar−CH_3), 3.14, 3.41 (s, 6H, *N*−CH_3), 4.11 (s, 2H, *S*-methyl), 5.58 (s, 2H, *N*-methyl), 7.05 (d, $J_{3',2'}$ = 6.4 Hz, 1H, *H*-3′), 7.25 (d, $J_{2',3'}$ = 6.4 Hz, 1H, H-2′), 7.31 (s, 1H, *H*-6′), 7.47−7.58 (m, 5H, Ar−*H*), 8.0 (s, 1H, HC═N), 10.16 (s, 1H, CO−amide). ^{13}C NMR, DMSO-d_6, 100 MHz, (δ/ppm): 19.23 (methyl), 20.06 (methyl), 27.93 (methyl), 29.90 (methyl), 37.39 (*S*-methylene), 41.33, (*N*-methylene), 106.46, 117.12, 120.78, 127.46 (3C), 130.06, 130.45, 130.76, 131.73, 132.40, 136.81, 136.93, 143.51, 148.40, 151.33, 151.70 (Ar−C), 151.77, 154.63 (2CO−xanthene), 165.43 (CO−amide). ES$^+$ MS (m/z %): 530.1849 (M$^+$). Anal. Calcd for $C_{26}H_{26}N_8O_3S$: C, 50.35; H, 3.60; N, 19.53. Found; C, 58.85; H, 4.94; N, 21.12.

*4.3.9. N-(4-Chlorophenyl)-2-(5-((1,3-dimethyl-2,6-dioxo-2,3-dihydro-1H-purin-7(6H)-yl)methyl)-4-phenyl-4H-1,2,4-triazol-3-ylthio)acetamide (**11i**).* Off-white solid; yield: 73%; mp 136 °C; IR (KBr) ν: 1600−1650 (2C═O), 3351 (N−H), 1643 (CONH), 1545 (N═C), 1473 (CH_2), Ph (1476), 1453 (C═C), 1331 (N−C), 600−700 (S−C), 801 (Ar−H). ^{1}H NMR, DMSO-d_6, 400 MHz, (δ/ppm): 3.13, 3.39 (s, 6H, *N*−CH_3), 4.14 (s, 2H, *S*-methylene), 5.57 (s, 2H, *N*-methylene), 7.33−7.56 (m, 9H, Ar−*H*), 7.99 (s, 1H, HC═N), 10.51 (s, 1H, CO−amide). ^{13}C NMR, DMSO-d_6, 100 MHz, (δ/ppm): 27.93 (methyl), 29.90 (methyl), 37.41 (*S*-methylene), 41.36, (*N*-methylene), 106.50, 119.56, 121.09, 123.99, 127.46−132.42 (11C), 139.20, 143.52 (2C), 148.41, 151.37, 151.64 (Ar−C), 151.80, 154.66 (2CO−xanthene), 165.75 (CO−amide). ES$^+$ MS (m/z %): 536.1146 (M$^+$). Anal. Calcd for $C_{24}H_{22}ClN_8O_3S$: C, 50.61; H, 3.88; N, 20.69. Found; C, 53.68; H, 3.94; N, 20.87.

*4.3.10. 2-(5-((1,3-Dimethyl-2,6-dioxo-2,3-dihydro-1H-purin-7(6H)-yl)methyl)-4-phenyl-4H-1,2,4-triazol-3-ylthio)-N-(2-fluorophenyl)acetamide (**11j**).* Light-brown solid; yield: 68%; mp 127 °C; IR (KBr) ν: 1600−1650 (2C═O), 3351 (N−H), 1643 (CONH), 1545 (N═C), 1473 (CH_2), Ph (1476), 1453 (C═C), 1331 (N−C), 600−700 (S−C), 801 (Ar−H). ^{1}H NMR, DMSO-d_6, 400 MHz, (δ/ppm): 3.15, 3.42 (s, 6H, *N*−CH_3), 4.19 (s, 2H, *S*-methylene), 5.58 (s, 2H, *N*-methylene), 7.19 (t, $J_{3',4'/4',5'}$ = 5.6 Hz, 1H, *H*-4′), 7.32 (t, $J_{5',6'/4',5'}$ = 6 Hz, 1H, *H*-5′), 7.48−7.58 (m, 6H, Ar−*H*), 7.77 (d, $J_{5',6'}$ = 6 Hz, 1H, *H*-6′), 8.0 (s, 1H, HC═N), 9.89 (s, 1H, CO−amide). ^{13}C NMR, DMSO-d_6, 100 MHz (δ/ppm): 27.93 (methyl), 29.90 (methyl), 37.41 (*S*-methylene), 41.36, (*N*-methylene), 106.50, 119.56, 121.09, 123.99, 127.46−132.42 (11C), 139.20, 143.52 (2C), 148.41, 151.37, 151.64 (Ar−C), 151.80, 154.66 (2CO−xanthene), 165.75 (CO−amide). ES$^+$ MS (m/z %): 520.1441 (M$^+$). Anal. Calcd for $C_{24}H_{22}FN_8O_3S$: C, 55.35; H, 3.90; N, 21.33. Found; C, 55.38; H, 4.07; N, 21.53.

4.4. MTT Assay. *4.4.1. Cell Culture.* The human MCF-7 breast and A549 lung cancer cell lines were cultured in Dulbecco's modified Eagle medium containing 10% fetal bovine serum and 1% streptomycin−penicillin (100 units/mL and 1% 100 μg/mL) at 37 °C having 5% carbon dioxide in a moistened atmosphere. Cell lines were treated with compounds in dimethyl sulfoxide (DMSO) (less than 1% final concentration).

4.4.2. Determination of Cell Viability. The cytotoxic prospective was evaluated by MTT assay. MCF-7 and A549 cells were sown in 96-well plates (microculture), and with different dilutions of compounds, cultured cells were supplemented for 48 h, following further incubation with 20 μL of MTT mixture (5 mg/mL) at 37 °C for 240 min. Later, formazan crystals were mixed in 150 μL of control (DMSO), and absorbance was quantified in a microplate reader at a wavelength of 490 nm and percentage cell viability was calculated.[48]

4.5. Hemolytic Assay. All the synthesized derivatives were examined following the literature[49] to find out their hemolytic potential. Blood samples (bovine) collected (3 mL) in EDTA were centrifuged at 1000 × *g* for 10 min. After the isolation of erythrocytes, it was washed three times with 5 mL of cold sterilized solution of PBS at 7.4 pH. The blood suspension (180 μL) was mixed with 20 μL of sample solution (10 mg/mL in negative control, *i.e.,* DMSO) and incubated for 30 min at 37 °C. ABTS and DMSO were used as positive and negative controls, respectively. At 576 nm absorbance of the sample, it was perceived to the % hemolysis was calculated.

$$\%\ \text{age of hemolysis} = [(\text{absorbance of test compound (sample)} - \text{absorbance of DMSO})/(\text{absorbance of ABTS})] \times 100$$

4.6. Computational Modeling Method. The *in silico* studies were executed to further delineate the mechanism of action of test compounds with higher pharmacological potential. The PASS prediction tool was utilized to predict the therapeutic target with 95% probability, and anti-cancer targets with probability of activity (Pa) > 50% were selected.[50] In the Molecular Operating Environment 2015.10, by the application of induced fit docking, the synthetic derivative was *in silico* docked against these targets. The compound was sketched and energy-minimized using the CHARMm force field with the MMFF9x partial charge in DS Visualizer 17.2. The conformer (3D) obtained with acefylline was (PubChem CID: 69550) retrieved from the database (PubChem). From PDB (Protein Data Bank) RSCB (http://www.rscb.org), the 3D X-ray structure (crystallized) of STAT3 (5AX3, 2.984 Å resolution) was retrieved. These structures were prepared by the Quickprep function of MOE to correct the structural problems such as missing residues, alternates, and terminus capping. The structures were protonated to resist the modification (molecular) of binding pose. The molecular system was energy-minimized with Amber10: EHT force field. The Site Finder application was used to identify and isolate the potential binding pocket at the hotspot of STAT3. The Dock function was used to place the compounds in the binding pocket with the triangle placement method (matcher) and recorded with London dG. Redocking was done and ranked with a scoring function (GBVI/WSA dG). The pose with the highest conformational energy (ΔG) was utilized to simulate the protein−ligand interactions in DS Visualizer 17.2. Acefylline served as a standard, and its binding score was used as a standard's threshold.

https://doi.org/10.1021/acsomega.1c00424
ACS Omega 2021, 6, 11943−11953

5. STATISTICAL DATA

All the measurements were carried out in triplicate, and statistical analysis was performed using Prism. The results are presented as mean ± SD.

■ ASSOCIATED CONTENT

Supporting Information

The Supporting Information is available free of charge at https://pubs.acs.org/doi/10.1021/acsomega.1c00424.

^{1}H NMR and ^{13}C NMR spectra of newly synthesized compounds **11a−j** (PDF)

■ AUTHOR INFORMATION

Corresponding Author

Ameer Fawad Zahoor − *Department of Chemistry, Government College University Faisalabad, Faisalabad 38000, Pakistan;* orcid.org/0000-0003-2127-8848; Email: fawad.zahoor@gcuf.edu.pk, fawad.zahoor@gmail.com

Authors

Irum Shahzadi − *Department of Chemistry, Government College University Faisalabad, Faisalabad 38000, Pakistan*

Azhar Rasul − *Department of Zoology, Government College University Faisalabad, Faisalabad 38000, Pakistan*

Asim Mansha − *Department of Chemistry, Government College University Faisalabad, Faisalabad 38000, Pakistan;* orcid.org/0000-0001-5659-0562

Sajjad Ahmad − *Department of Chemistry, University of Engineering and Technology Lahore, Faisalabad 38000, Pakistan*

Zohaib Raza − *Department of Pharmacology, Government College University Faisalabad, Faisalabad 38000, Pakistan*

Complete contact information is available at: https://pubs.acs.org/10.1021/acsomega.1c00424

Notes

The authors declare no competing financial interest.

■ ACKNOWLEDGMENTS

The authors are thankful to Government College University Faisalabad, UET Lahore FSD Campus and to HEC for providing funding under the NRPU project 8702 for facilitating to carry out work.

■ REFERENCES

(1) Sudhakar, A. History of Cancer, Ancient and modern treatment methods. *J Canc Sci Ther* **2009**, *01*, i−iv.

(2) Ruddarraju, R. R.; Murugulla, A. C.; Kotla, R.; Tirumalasetty, M. C. B.; Wudayagiri, R.; Donthabakthuni, S.; Maroju, R.; Maroju, R. Design, synthesis, anticancer activity and docking studies of theophylline containing 1,2,3-triazoles with variant amide derivatives. *Med. Chem. Commun.* **2016**, *8*, 176−183.

(3) Hassanpour, S. H.; Dehghani, M. Review of cancer from perspective of molecular. *Journal of Cancer Research and Practice* **2017**, *4*, 127−129.

(4) Arruebo, M.; Vilaboa, N.; Sáez-Gutierrez, B.; Lambea, J.; Tres, A.; Valladares, M.; González-Fernández, Á. Assessment of the evolution of cancer treatment therapies. *Cancers* **2011**, *3*, 3279−3330.

(5) Prachayasittikul, V.; Pingaew, R.; Anuwongcharoen, N.; Worachartcheewan, A.; Nantasenamat, C.; Prachayasittikul, S.; Ruchirawat, S.; Prachayasittikul, V. Discovery of novel 1,2,3-triazole derivatives as anticancer agents using QSAR and in silico structural modification. *Springerplus* **2015**, *4*, 571−592.

(6) Holla, B. S.; Mahalinga, M.; Karthikeyan, M. S.; Poojary, B.; Akberali, P. M.; Kumari, N. S. Synthesis, characterization and antimicrobial activity of some substituted 1,2,3-triazoles. *European Journal of Medicinal Chemistry* **2005**, *40*, 1173−1178.

(7) Sanghvi, Y. S.; Bhattacharya, B. K.; Kini, G. D.; Matsumoto, S. S.; Larson, S. B.; Jolley, W. B.; Robins, R. K.; Revankar, G. R. Growth inhibition and induction of cellular differentiation of human myeloid leukemia cells in culture by carbamoyl congeners of ribavirin. *J. Med. Chem.* **1990**, *33*, 336−344.

(8) Hafez, H. N.; Abbas, H. A.; El-Gazzar, A. R. Synthesis and evaluation of analgesic, anti-inflammatory and ulcerogenic activities of some triazolo- and 2-pyrazolyl-pyrido [2,3-d]-pyrimidines. *Acta Pharm.* **2008**, *58*, 359−378.

(9) Chen, M.; Lu, S.; Yuag, G.; Yang, S.; Du, X. Synthesis and antimicrobial activity of some heterocyclic beta-enamino ester derivatives with 1,2,3-triazole. *Heterocycl. Commun.* **2000**, *6*, 421−426.

(10) Sheremet, E. A.; Tomanov, R. I.; Trukhin, E. V.; Berestovitskaya, V. M. Synthesis of 4-Aryl-5-Nitro-1,2,3-Triazoles. *Russ. J. Org. Chem.* **2004**, *40*, 594−595.

(11) Banu, K. M.; Dinaker, A.; Ananthnarayan, C. Synthesis, characterization of antimicrobial studies and pharmacological screening of some substituted 1,2,3-triazoles. *Indian J. Pharm. Sci.* **1999**, *61*, 202−205.

(12) Gujjar, R.; Marwaha, A.; El Mazouni, F.; White, J.; White, K. L.; Creason, S.; Shackleford, D. M.; Baldwin, J.; Charman, W. N.; Buckner, F. S.; Charman, S.; Rathod, P. K.; Phillips, M. A. Identification of a Metabolically Stable Triazolopyrimidine-Based Dihydroorotate Dehydrogenase Inhibitor with Antimalarial Activity in Mice. *J. Med. Chem.* **2009**, *52*, 1864−1872.

(13) Guan, L.-P.; Jin, Q.-H.; Tian, G.-R.; Chai, K.-Y.; Quan, Z.-S. Synthesis of some quinoline-2(1*H*)-one and 1,2,4-Triazolo [4,3-a]quinoline derivatives as potent anticonvulsants. *J. Pharm. Sci.* **2007**, *10*, 254−262.

(14) Johns, B. A.; Weatherhead, J. G.; Allen, S. H.; Thompson, J. B.; Garvey, E. P.; Foster, S. A.; Jeffrey, J. L.; Miller, W. H. The use of oxadiazole and triazole substituted naphthyridines as HIV-1 integrase inhibitors. Part 1: Establishing the pharmacophore. *Bioorganic & Medicinal Chemistry Letters* **2009**, *19*, 1802−1806.

(15) Passannanti, A.; Diana, P.; Barraja, P.; Mingooia, F.; Lauria, A.; Cirrincine, G. Pyrrolo[2,3-d][1,2,3]triazoles as potential antineoplastic agents. *Heterocycles* **1998**, *48*, 1229−1235.

(16) Duran, A.; Dogan, H. N.; Rollas, S. Synthesis and preliminary anticancer activity of new 1,4-dihydro-3-(3-hydroxy-2-naphthyl)-4-substituted-5H-1,2,4-triazoline-5-thiones. *Il Farmaco* **2002**, *57*, 559−564.

(17) Kharb, R.; Sharma, P. C.; Yar, M. S. Pharmacological significance of triazole scaffold. *J. Enzyme Inhib. Med. Chem.* **2011**, *26*, 1−21.

(18) Xu, Z.; Zhao, S.-J.; Liu, Y. 1,2,3-Triazole-containing hybrids as potential anticancer agents: Current developments, action mechanisms and structure-activity relationships. *European Journal of Medicinal Chemistry* **2019**, *183*, 111700−111737.

(19) Mahanti, S.; Sunkara, S.; Bhavani, R. Synthesis, biological evaluation and computational studies of fused acridine containing 1,2,4-triazole derivatives as anticancer agents. *Synthetic Communications* **2019**, *49*, 1729−1740.

(20) Marx, D.; Wingen, L. M.; Schnakenburg, G.; Müller, C. E.; Scholz, M. S. Fast, efficient, and versatile synthesis of 6-amino-5-carboxamidouracils as precursors for 8-substituted xanthines. *Front. Chem.* **2019**, *7*, 1−15.

(21) Singh, N.; Shreshtha, A. K.; Thakur, M. S.; Patra, S. Xanthine scaffold: scope and potential in drug development. *Heliyon* **2018**, *4*, No. e00829.

(22) Rogliani, P.; Calzetta, L.; Ora, J.; Cazzola, M.; Matera, M. G. Efficacy and safety profile of doxofylline compared to theophylline in asthma: a meta-analysis. *Multidiscip. Respir. Med.* **2019**, *14*, 1−8.

(23) Barnes, P. J. Theophylline. *Pharmaceuticals* **2010**, *3*, 725−747.

(24) Chang, Y.-L.; Hsu, Y.-J.; Chen, Y.; Wang, Y.-W.; Huang, S.-M. Theophylline exhibits anti-cancer activity *via* suppressing SRSF3 in cervical and breast cancer cell lines. *Oncotarget* **2017**, *8*, 101461−101474.
(25) Yousaf, M.; Zahoor, A. F.; Faiz, S.; Javed, S.; Irfan, M. Recent synthetic approaches towards biologically potent derivatives/analogues of theophylline. *J. Heterocyclic Chem.* **2018**, *55*, 2447−2479.
(26) Monteiro, J.; Alves, M.; Oliveira, P.; Silva, B. Structure-bioactivity relationships of methylxanthines: Trying to make sense of all the promises and the drawbacks. *Molecules* **2016**, *21*, 974−1005.
(27) Barnes, P. J. Theophylline. *Am. J. Respir. Crit. Care Med.* **2013**, *188*, 901−906.
(28) Hayallah, A. K. M.; Talhouni, A. A.; Alim, A. A. M. A. Design and synthesis of new 8-anilide theophylline derivatives as bronchodilators and antibacterial agents. *Arch. Pharm. Res.* **2012**, *35*, 1355−1368.
(29) Mangasuli, S. N.; Hosamani, K. M.; Devarajegowda, H. C.; Kurjogi, M. M.; Joshi, S. D. Synthesis of coumarin-theophylline hybrids as a new class of anti-tubercular and anti-microbial agents. *Eur. J. Med. Chem.* **2018**, *146*, 747−756.
(30) Cegla, M. T.; Potaczek, J.; Zylewski, M.; Strekowski, L. Synthesis of the hypotensive agent 8-amino-7-[2-hydroxy-3-morpholinopropyl]theophylline (P23) and analogs. *J. Heterocyclic Chem.* **2009**, *46*, 191−194.
(31) Alafeefy, A. M.; Alqasoumi, S. I.; Abdel hamid, S. G.; El-Tahir, K. E. H.; Mohamed, M.; Zain, M. E.; Awaad, A. S. Synthesis and hypoglycemic activity of some new theophylline derivatives. *J. Enzyme Inhib. Med. Chem.* **2014**, *29*, 443−448.
(32) Voynikov, Y.; Momekov, G.; Peikov, P. I.; Stavrakov, G. Cytotoxcity assay on several theophyllne-7-acetic acid amides with amino acids. *Pharmacia* **2014**, *61*, 12−16.
(33) Rico-Gómez, R.; López-Romero, J. M.; Hierrezuelo, J.; Brea, J.; Loza, M. I.; Pérez-González, M. Synthesis of new mannosyl, galactosyl and glucosyl theophylline nucleosides with potential activity as antagonists of adenosine receptors. DEMA-induced cyclization of glycosylideneiminouracils. *Carbohydrate Research* **2008**, *343*, 855−864.
(34) Szentmiklósi, A. J.; Cseppent, A.; Gesztelyi, R.; Zsuga, J.; Kortvely, A.; Harmati, A.; Nanasi, P. P. Xanthine derivatives in the heart: Blessed or cursed? *Curr. Med. Chem.* **2011**, *18*, 3695−3706.
(35) Foppoli, A.; Zema, L.; Gazzaniga, A.; Caira, M. R.; Nassimbeni, L. R.; Borkum, E.; Bettini, R.; Giordano, F. Solid-state chemistry of ambroxol theophylline-7-acetate. *Journal of Pharmaceutical Sciences* **2007**, *96*, 1139−1146.
(36) Voynikov, Y.; Valcheva, V.; Momekov, G.; Peikov, P.; Stavrakov, G. Theophylline-7-acetic acid derivatives with amino acids as anti-tuberculosis agents. *Bioorganic & Medicinal Chemistry Letters* **2014**, *24*, 3043−3045.
(37) Stavrakov, G.; Valcheva, V.; Voynikov, Y.; Philipova, I.; Atanasova, M.; Konstantinov, S.; Peikov, P.; Doytchinova, I. Design, synthesis, and antimycobacterial activity of novel theophylline-7-acetic acid derivatives with amino acid moieties. *Chem. Biol. Drug Des.* **2016**, *87*, 335−341.
(38) Zlatkov, A. B.; Peikov, P. T.; Momekov, G. C.; Pencheva, I.; Tsvetkova, B. Synthesis, stability and computational study of some ester derivatives of theophylline-7-acetic acid with antiproliferative activity. *Der. Pharma. Chem.* **2010**, *2*, 197−210.
(39) Shahzadi, I.; Zahoor, A. F.; Rasul, A.; Rasool, N.; Raza, Z.; Faisal, S.; Parveen, B.; Kamal, S.; Zia-ur-Rehman, M.; Zahid, F. M. Synthesis, anticancer, and computational studies of 1, 3, 4-oxadiazole-purine derivatives. *J Heterocyclic Chem* **2020**, *57*, 2782−2794.
(40) Faiz, S.; Zahoor, A. F.; Ajmal, M.; Kamal, S.; Ahmad, S.; Abdelgawad, A. M.; Elnaggar, M. E. Design, Synthesis, Antimicrobial Evaluation, and Laccase Catalysis Effect of Novel Benzofuran-Oxadiazole and Benzofuran-Triazole Hybrids. *J. Heterocyclic Chem.* **2019**, *56*, 2839−2852.
(41) Akhtar, R.; Zahoor, A. F.; Rasul, A.; Ahmad, M.; Anjum, M. N.; Ajmal, M.; Raza, Z. Design, synthesis, *In-silico* study and anti-cancer potential of novel *n*-4-piperazinyl-ciprofloxacin-aniline hybrids. *Pak. J. Pharm. Sci.* **2019**, *32*, 2215−2222.
(42) Sharba, A.; Al-Bayati, R.; Aouad, M.; Rezki, N. Synthesis of oxadiazoles, thiadiazoles and triazoles derived from benzo[b]-thiophene. *Molecules* **2005**, *10*, 1161−1168.
(43) Cormier, R.; Burda, W. N.; Harrington, L.; Edlinger, J.; Kodigepalli, K. M.; Thomas, J.; Kapolka, R.; Roma, G.; Anderson, B. E.; Turos, E.; Shaw, L. N. Studies on the Antimicrobial Properties of *N*-acylated ciprofloxacins. *Bioorganic & Medicinal Chemistry Letters* **2012**, *22*, 6513−6520.
(44) Johnston, P. A.; Grandis, J. R. STAT3 signaling: anti-cancer strategies and challenges. *Mol. Interventions* **2011**, *11*, 18−26.
(45) Gaafer, A. G. A.; Messiha, B. A. S.; Abdelkefy, A. M. L. Nicorandil and theophylline can protect experimental rats against complete freund's adjuvant-induced Rheumatoid Arthritis through modulation of JAK/STAT/RANKL signaling pathway. *Eur. J. Pharmacol.* **2018**, *822*, 177−185.
(46) Washburn, K. B.; Neary, J. T. P2 purinergic receptors signal to STAT3 in astrocytes: Difference in STAT3 responses to P2Y and P2X receptor activation. *Neuroscience* **2006**, *142*, 411−423.
(47) Xu, J.; Sylvester, R.; Tighe, A. P.; Chen, S.; Gudas, L. J. Transcriptional activation of the suppressor of cytokine signaling-3 (SOCS-3) Gene via STAT3 is increased in F9 REX1 (ZFP-42) knockout teratocarcinoma stem cells relative to wild-type cells. *Journal of Molecular Biology* **2008**, *377*, 28−46.
(48) Rasul, A.; Di, J.; Millimouno, F.; Malhi, M.; Tsuji, I.; Ali, M.; Li, J.; Li, X. Reactive oxygen species mediate isoalantolactone-induced apoptosis in human prostate cancer cells. *Molecules* **2013**, *18*, 9382−9396.
(49) Riaz, M.; Rasool, N.; Bukhari, I.; Shahid, M.; Zubair, M.; Rizwan, K.; Rashid, U. In Vitro antimicrobial, antioxidant, cytotoxicity and GC-MS analysis of *Mazus goodenifolius*. *Molecules* **2012**, *17*, 14275−14287.
(50) Parasuraman, S. Prediction of activity spectra for substances. *J. Pharmacol. Pharmacother.* **2011**, *2*, 52−53.

https://doi.org/10.1021/acsomega.1c00424
ACS Omega 2021, 6, 11943−11953